

Supporting Information

The first examples of lanthanide selenite-carboxylate compounds: syntheses, crystal structures and properties

Xiao-Feng Guo, Mei-Ling Feng, Zai-Lai Xie, Jian-Rong Li, and Xiao-Ying Huang*

State Key Laboratory of Structural Chemistry, Fujian Institute of Research on the Structure of Matter, Chinese Academy of Sciences, Fuzhou, Fujian 350002, P. R. China, E-mail: xyhuang@ffjirsm.ac.cn

1. More Structural details

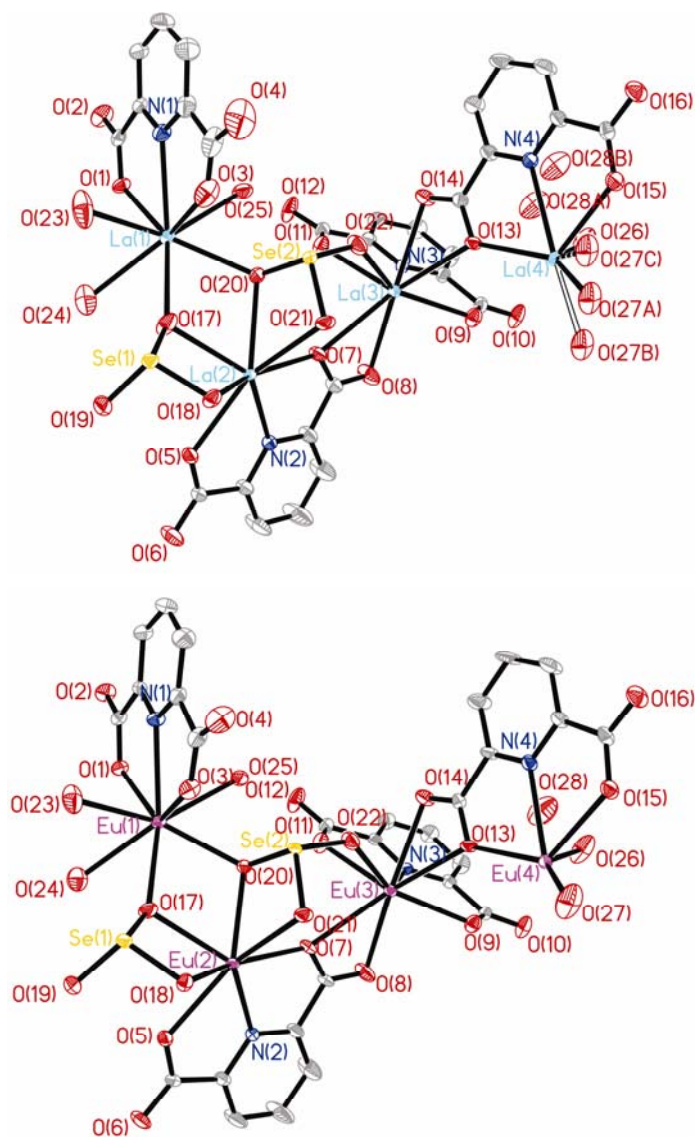


Fig. S1 ORTEP plots of the crystallographically asymmetric units in **1** (top) and **3** (bottom); thermal ellipsoids are given at the 50% probability level; hydrogen atoms are omitted for clarity.

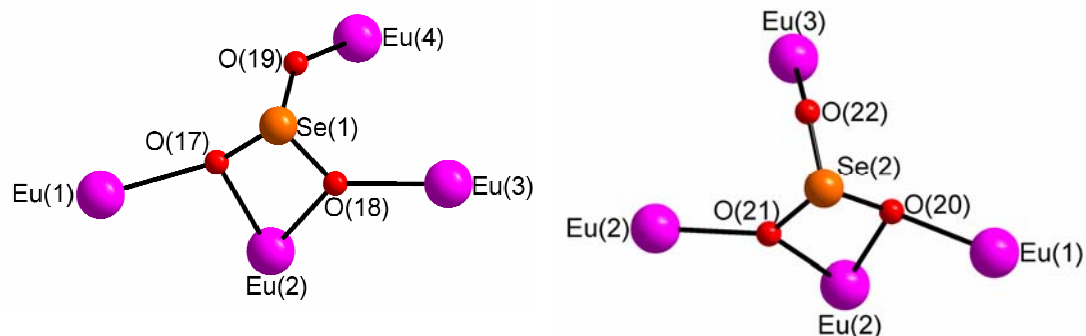


Fig. S2 Coordination modes of SeO_3 groups. The Se(1)O_3 group chelates with the Eu(2) ion and bridges to three other Eu(III) ions, Eu(1) , Eu(3) , Eu(4) ; whereas Se(2)O_3 chelates with the Eu(2) ion and bridges to Eu(1) , Eu(2) , Eu(3) ions.

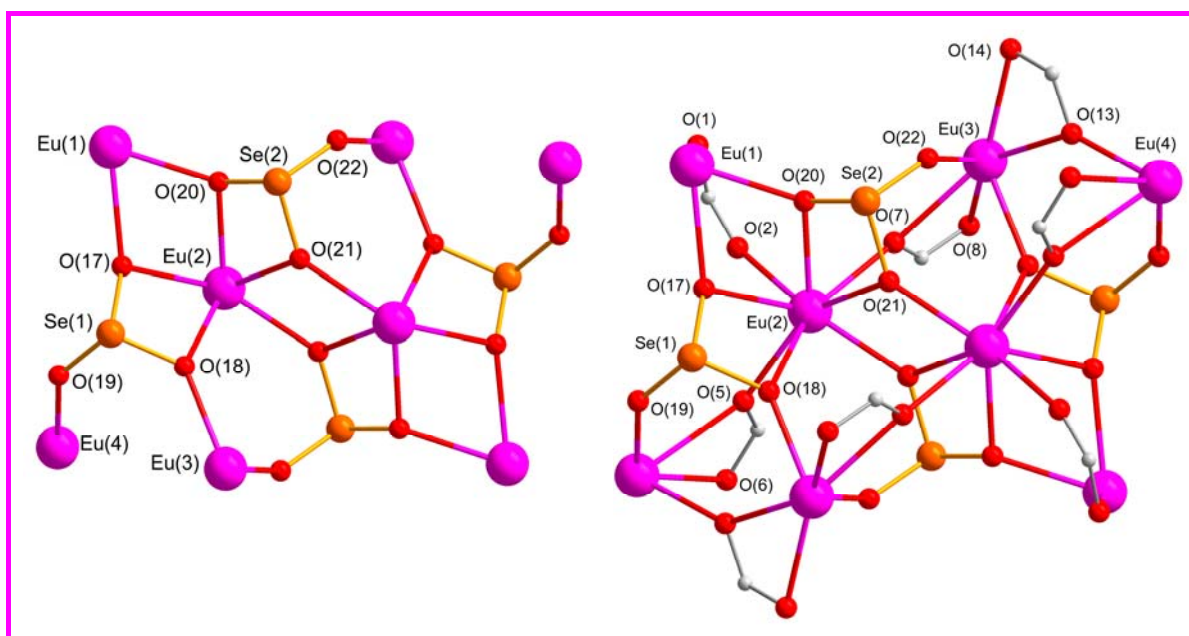


Fig. S3 Left: The $\text{Eu}_8(\text{SeO}_3)_4$ core in the cluster. Right: A plot showing that the Eu pairs in the cluster are connected by both SeO_3^{2-} and CO_2^- groups.

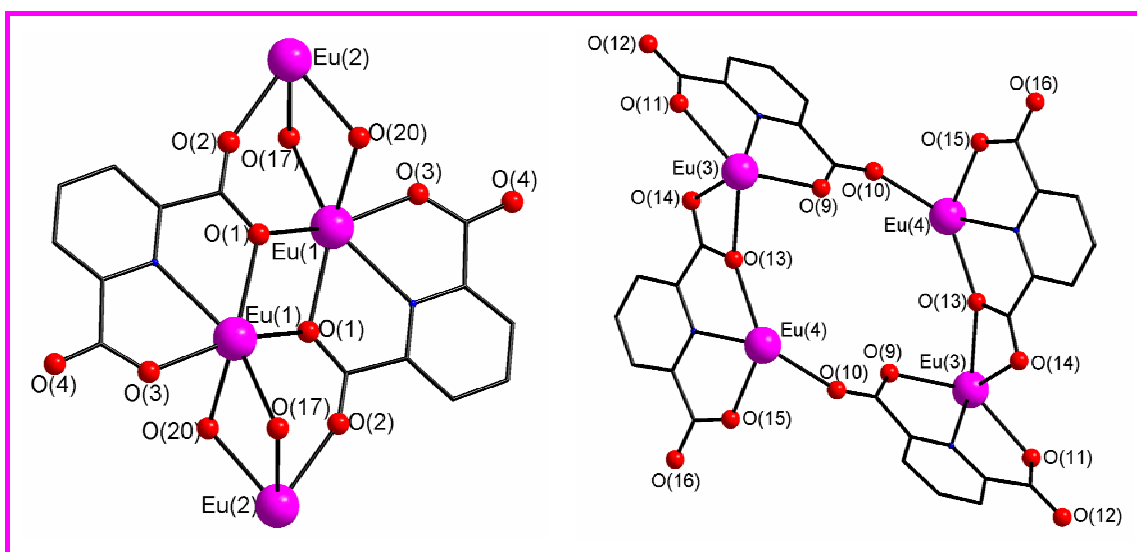


Fig. S4 The Eu_2O_2 rhombic unit (left) and $\text{Eu}_4\text{O}_2(\text{COO})_2$ 12-membered ring (right) in **3** which connect the clusters into an extended 2D-network along b axis and c axis, respectively.

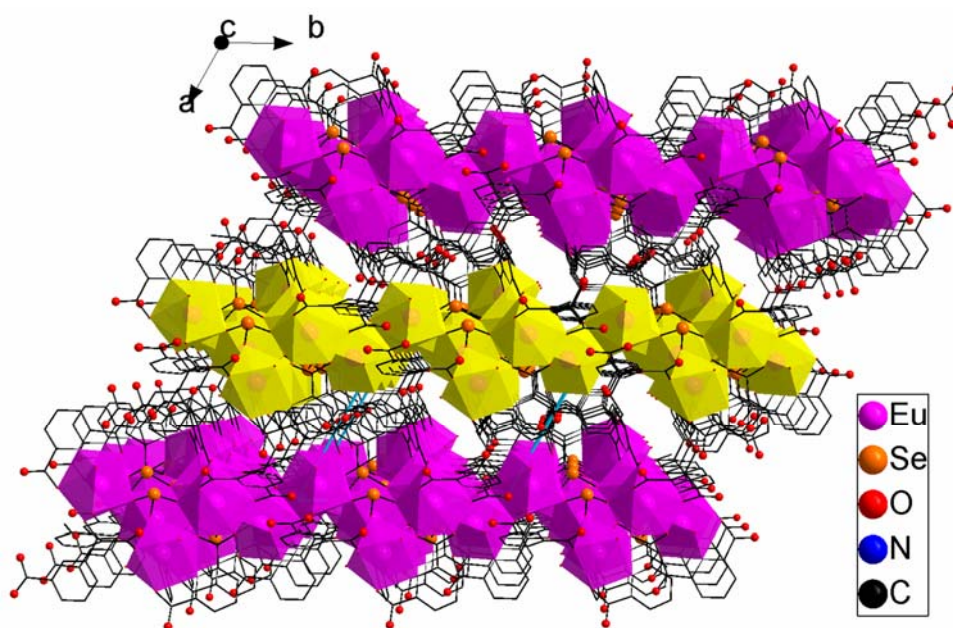


Fig. S5 Polyhedral view of the packing of layers in compound **3** down the c -axis. One of the layers is highlighted in yellow for clarity.

2. Physical measurements.

2a) IR spectra

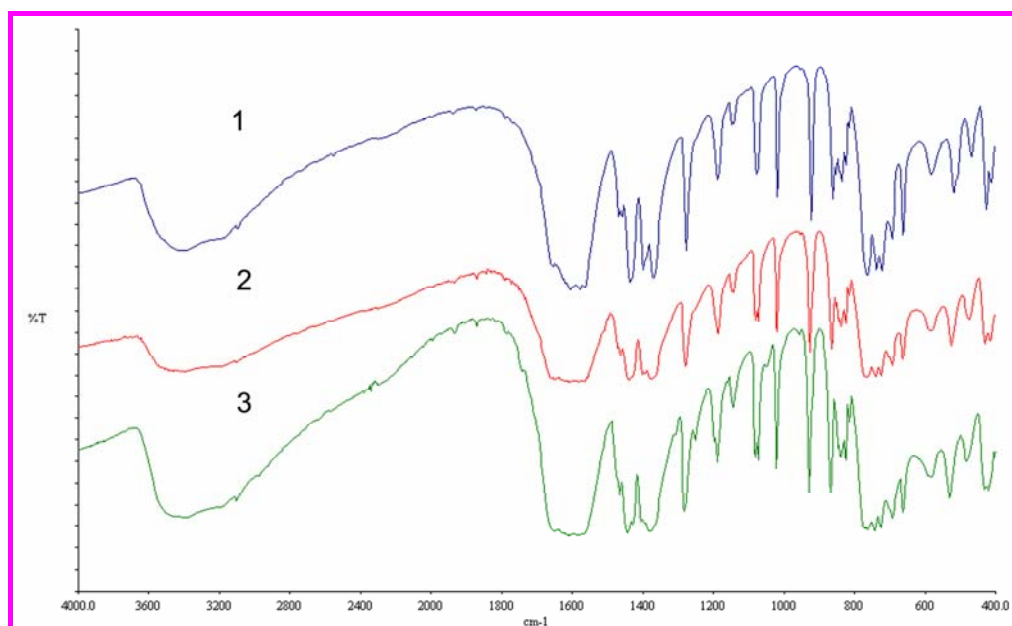


Fig. S6 IR Spectra of compounds **1** (La), **2** (Nd) and **3** (Eu).

2b) PXRD

Powder X-ray diffraction patterns were recorded on a Rigaku Dmax/2500 diffractometer using CuK α radiation in the angular range of $2\theta = 2-50^\circ$.

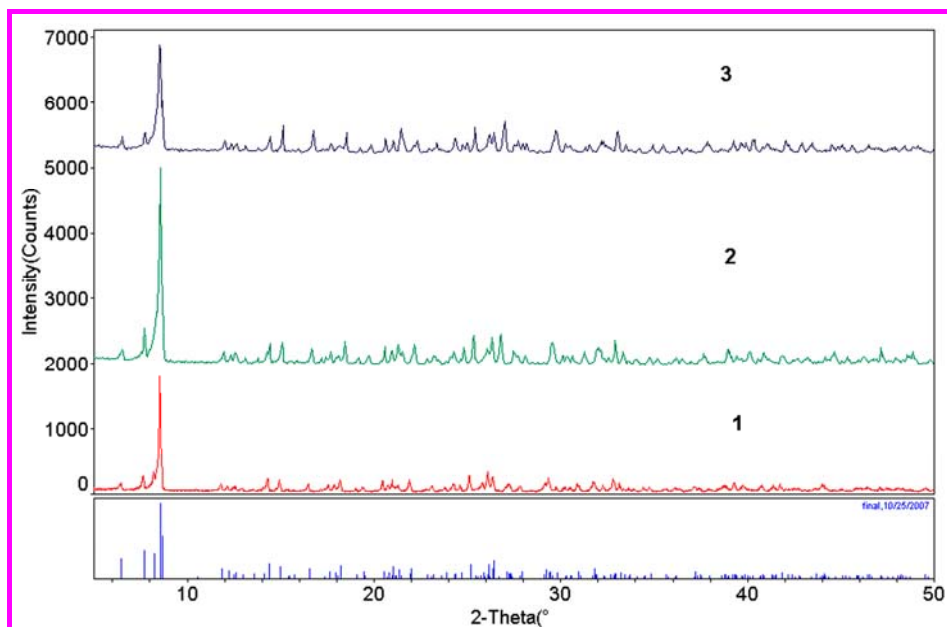


Fig. S7 The PXRD patterns of compounds **1** (La), **2** (Nd) and **3** (Eu) are in very good agreement with the simulated PXRD pattern calculated from single crystal X-ray data of **3** (bottom), indicating the phase purity of **1** (La), **2** (Nd) and **3** (Eu).

3. Dehydration and rehydration process

Thermogravimetric analyses (TGA) were carried out on a METTLER TGA/SDTA851e thermal analyzer from room temperature to 300°C in a ramp rate of 20°C/min and constant temperature at 300°C for approximate 30 mins in a dynamic dry air atmosphere. Powder X-ray diffraction patterns were recorded on a Rigaku Dmax/2500 diffractometer using CuK α radiation in the angular range of $2\theta = 2-50^\circ$.

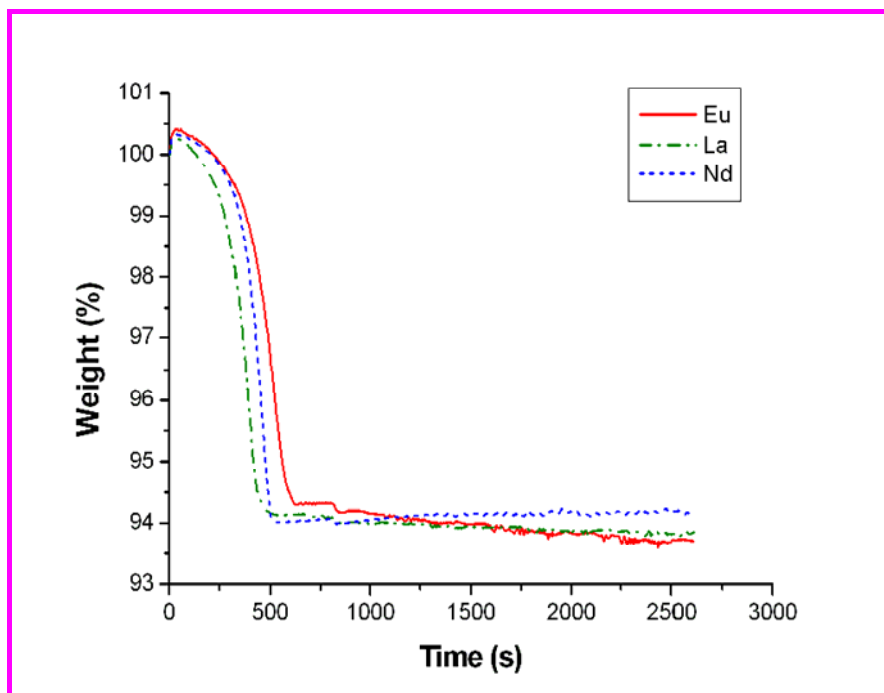


Fig S8. The dehydration process of **1** (La), **2** (Nd), and **3** (Eu).

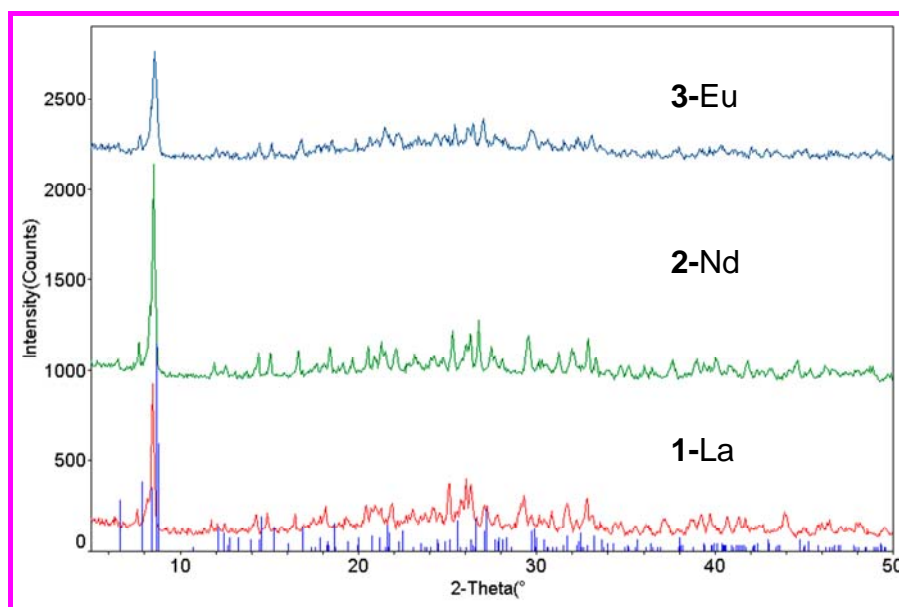


Fig. S9 Room temperature PXRD patterns for residual of **1** (La), **2** (Nd), and **3** (Eu) after heating at 300°C for approximate 30 mins; the simulated PXRD pattern from single crystal X-ray data of **3** (Eu) was plotted at the bottom for comparison.

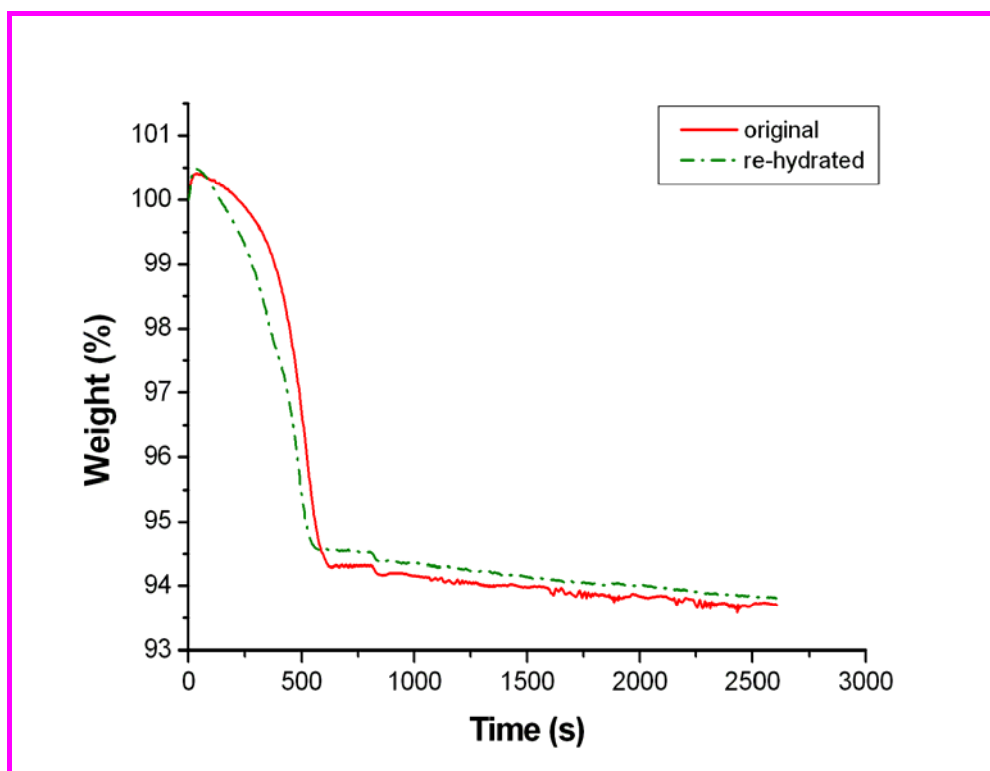


Fig. S10 The dehydration process of **3** (Eu) by heating at 300 °C for approximate 30 mins. The red curve showed the dehydration process of the original sample. The green curve showed the dehydration process of the rehydrated sample of **3** (Eu) by being exposed to air for twelve days.

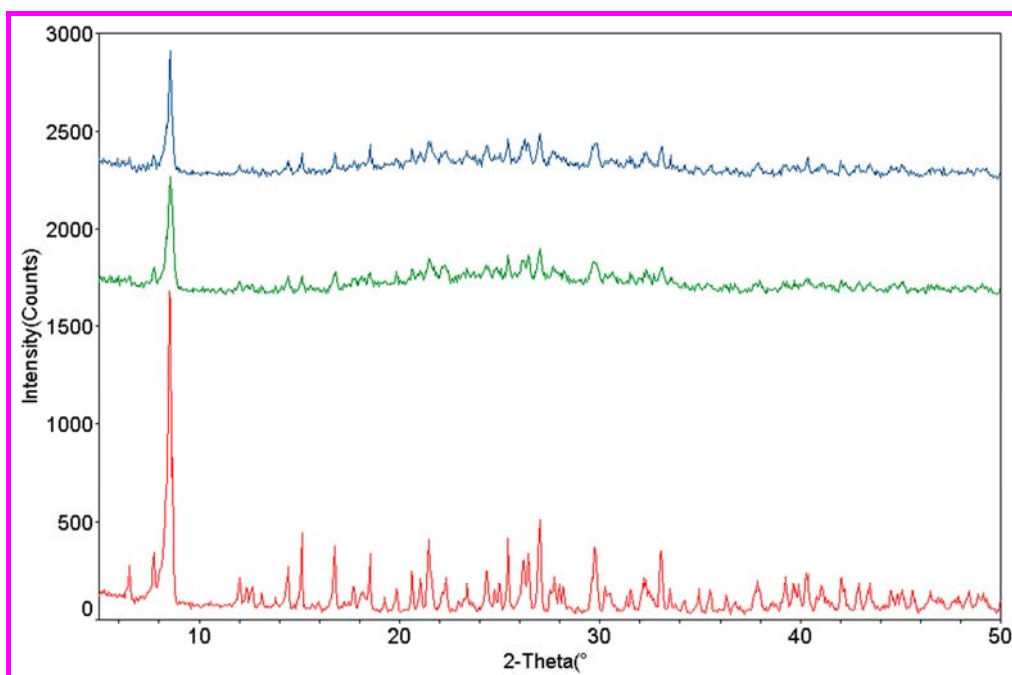


Fig. S11 Room temperature PXR patterns of the TGA residual of **3** (Eu). The middle one is for the residue of **3** (Eu) right after heating at 300°C for approximate 30 mins. The residue was rehydrated by being exposed to air for twelve days. The rehydrated sample was heated at 300 °C for approximate 30 mins and the PXR of the residue was shown at the top. The PXR pattern of the original pure sample of **3** (Eu) is plotted at the bottom for comparison.